ROBUST STABILIZATION OF A TRANSONIC FLUTTER BASED ON A LINEARIZED TRANSONIC MATH MODEL

Hiroshi Matsushita, Kenichi Saitoh, and Masataka Hashidate,
National Aerospace Laboratory
Tokyo, Japan

To get much benefit of simplicity from the linear control, a transonic aerodynamics is linearized to obtain a linear aeroelastic math model and the robust control design method is applied to yield linear control laws. An aeroelastic model of high aspect ratio wing with a leading and a trailing edge control surface was designed and fabricated in order to investigate the applicability of active control to manage a transonic flutter. Flutter tests were carried out in the transonic wind tunnel at the National Aerospace Laboratory and the model exhibited a typical transonic nonlinear phenomena such as a transonic dip and a limit cycle oscillation. A transonic full potential code, USTF3, is extended to calculate the generalized aerodynamic forces due to eigen mode oscillation and linear approximation is carried out by getting a describing function and fitting a linear finite state aerodynamic model to the calculated data. Since a finite state linearized model has many sources of modeling error, the H_∞ loop-shaping method with the normalized left coprime factors approach is applied to provide a stability robustness against model uncertainty. The sensitivity analysis conducted for the resulting 7th-order controller exhibits robustness and the comparison with the laws which were designed based on a subsonic code and tested in the wind tunnel shows promising results for this newly designed laws as well.

Introduction

Active control of aeroelastic phenomena such as gust load response and flutter provides great benefit to vehicle safety, energy efficiency and flight performance. Research efforts for more than a decade at NAL have established the design methodology of these active control systems in the low subsonic speed range.[1] It still remains however to extend the technology towards a transonic region where flutter dynamic pressure drops significantly, known as the transonic dip phenomenon.[2], [3]

Due to a shock wave staying on a wing surface, steady and unsteady transonic aerodynamic forces are nonlinearly dependent on angle of attack or oscillation amplitude. Transonic flutter, therefore, often behaves like nonlinear and is difficult to be expressed with a simple linear mathematical formulation. However, the linearized unsteady aerodynamics still provide a good estimation for a transonic flutter even though the static or steady state aerodynamics are nonlinear.[4] As a first step to verify the promise and limitation in applying linear subsonic aerodynamics, robust stabilization method was tried to get a control law to suppress flutter. The control laws were implemented in the wing model and tested in the wind tunnel resulting the increment of 11.4 % in the flutter dynamic pressure.[5]-[7] While the robust stability method was thus validated its promise against the nonlinear characteristics of transonic flutter, the research effort to refine the math model by using a transonic code is still necessary as the next step.

Previously, limited numbers of research were carried out on designing control laws based directly on transonic aerodynamics. Batina et al tried to apply transonic codes to aeroelastic modeling of 2 dimensional wing and investigate possible flutter speed increment with a simple feedback control.[8] They showed that almost the same procedure as applied to subsonic region can also be applied to a transonic region.

Present study tries to extend their work to three dimensional transonic full potential code USTF3, which was developed by Isogai.[9] Since a finite state linearized model has many sources of modeling error such as linear approximation and mode truncation, the H_∞ loop-shaping method with the normalized left coprime factors approach is applied as a control law design method which will provide a stability robustness against model uncertainty.

Linearization of Transonic Aerodynamics

Mathematical modeling procedure to get linear model approximating transonic aerodynamic forces is almost parallel to subsonic analysis. With an expression of a flexible wing deformation $z(x,y,t)$ by N structural modes, $z_{qi}(x,y)$, and two control surface modes $z_{\delta j}(x,y)$ such as

$$z(x,y,t) = \sum_{i=1}^{N} z_{qi}(x,y)q_i(t) + \sum_{j=1}^{2} z_{\delta j}(x,y)\delta_j(t) \qquad (1)$$

fundamental equations for aeroelastic wing is expressed as[10),(11)].

$$M\ddot{q} + B_c\dot{q} + Kq + S\ddot{\delta} = f_a \qquad (2)$$

where M,, B_c, and K are mass matrix, damping matrix, and stiffness matrix, respectively; $q_i(t)$ and $\delta_j(t)$ are the generalized coordinates and control surface deflection, respectively. The last term on the left hand side of Eq.(2) is an inertial coupling term; s_{ij} represents the inertial force coefficient on the i-th mode due to j-th control surface activity.

The terms f_a on the right hand side of Eq.(2) are generalized aerodynamic forces due to aircraft motion. Since we treat here transonic aerodynamics which behaves nonlinearly, they can be expressed at most symbolically by aerodynamic operator for generalized coordinates. When we linearize the transonic aerodynamics for small disturbance condition, they can be expressed using aerodynamic influence matrix $F_a(k,M)$ as,

$$f_a = F_a(k,M)\, q \qquad (3a)$$

and the elements of $F_a(k,M) = \{ f_{aij} \}$ are defined by the pressure distribution caused by j-th eigen mode oscillation $\Delta p_{aj}(x,y;k,M)$ such that

$$f_{aij} = \iint_S \Delta p_{aj}(x,y;k,M)\, z_{qi}(x,y)dxdy \qquad (3b)$$

The pressure distributions in Eq. (3b) are calculated for each eigen mode oscillation at specific Mach number M and reduced frequency $k=b_0\omega/U$ where b_0, ω, U being a half mean aerodynamic chord, circular frequency and flow velocity, respectively.

Because of nonlinear nature of transonic aerodynamics, the time response of the generalized aerodynamic forces, $f_a(t)$, due to harmonic oscillation of eigen mode will contain higher harmonic components; it is necessary to take a fundamental component of the Fourier series expansion of generalized aerodynamic forces response at each frequency to get a describing function for transonic aerodynamics.

In order to design a control law for active flutter suppression, transonic describing functions have to be further approximated by a set of linear differential equations which is called a state-space equation of finite dimension. Specifically, the linear finite dimensional equation of the generalized aerodynamic forces should be expressed by the following:

$$f_a(t) = A_2 (\ddot{q}(t)^T \delta(t)^T)^T + A_1 (\dot{q}(t)^T \delta(t)^T)^T + A_0 (q(t)^T \delta(t)^T)^T + r(t) \qquad (4a)$$

$$\dot{r}(t) = \Lambda r(t) + B_0 (q(t)^T \delta(t)^T)^T \qquad (4b)$$

where $\Lambda = diag(-\lambda, \ldots, -\lambda)$

with the Fourier transformation counterparts to this expression in a frequency domain as follows.

$$F_a(k) = A(k)\ (q(k)^T \delta^T)^T \qquad (5a)$$

$$A(k) = (ik)^2[A_{2q}\ A_{2\delta}] + (ik)[A_{1q}\ A_{1\delta}] + [A_{0q}\ A_{0\delta}] + \frac{[B_{0q}\ B_{0\delta}]}{ik + \lambda} \qquad (5b)$$

Mathematical model coefficients A_0's, A_1's, A_2's and B_0's are obtained by least square error curve fitting in frequency domain to aerodynamic describing functions, $F_a(k)$

Once we get a linear formulation for the transonic aerodynamics, we can follow the routine procedure to get the whole equations in the state space form. Making use of the finite state expression for unsteady aerodynamics, Eq.(4), along with the second order expression for control actuator dynamics such as

$$\ddot{\delta} + C_\delta\dot{\delta} + K_\delta\delta = K_\delta\delta_c \qquad (6)$$

where control command $\delta_c = (\delta_{c1}, \delta_{c2})^T$, fundamental aeroelastic equation (2) can be transformed to state equation such as

$$\dot{x}(t) = Ax(t) + Bu(t) + w(t) \qquad (7)$$

where a state variable vector is defined as $x = (\dot{q}^T, \delta^T, q^T, \delta^T, r^T, w_g)^T$ and a control variable vector u contains the control commands. A system noise w introduced at the right hand side of the equation represents some noise source and is assumed as a white noise.

The observable output which can be used as a feedback signal, such as an accelerometer, a wing spar strain, etc, can be expressed by linear combination of the state and control variables as

$$y(t) = Cx(t) + Du(t) + v(t) \qquad (8)$$

with v being a measurement noise.

Numerical Analysis by USTF3 Code

Transonic aeroelastic wing model

We refurnished a transonic flutter model which was previously used to study a transonic flutter characteristics of a supercritical wing[12]. We installed a leading- and a trailing-edge control surfaces which are activated by electric geared motor. Since the torque needed to control the surface was estimated too high, the mid part of the wing is inflated so that it contains the motors of rather large size. The baseline wing has a supercritical wing section, while at an inflated part, symmetrical thick wing section is used.

The inflated part is composed of five sets of rigid plastic covers which are attached to a wing spar made by aluminum alloy, so as not to influence the original rigidity of the wing. We call these part as a glove. The plan form of the model is shown in Fig. 1. The structural model which characterizes vibration frequency and mode is derived by FEM analysis and a ground vibration test. The first four modes are as shown in Fig. 2.

Flutter tests were also conducted and revealed a typical transonic dip phenomena with the dip Mach number of 0.81 as shown in Fig. 3, and limit cycle oscillation was observed as shown in Fig. 4. It is worth notifying that the original wing (without control surfaces and inflated glove part) also had a limit cycle tendency and a transonic dip ; so fundamental flutter characteristics are retained by refurbishment.

Steady transonic analysis

Steady and unsteady analysis of the transonic flow around the model were carried out using USTF3 code installed in NAL supercomputer, Numerical Wind Tunnel (NWT). NWT is comprised of 140 processing elements (PE), with 1.5 GFLOPS performance each, and has a total peak performance of 236 GFLOPS. One PE was used in the present calculation.

In Fig. 5, the grid systems in xy plane (wing section plane) and in xz plane (wing planform plane) are shown. The total number of grid points in case of flap aerodynamics calculation are 47×31×23 for x, y, and z direction, respectively, in which 8×3 points are on the flap.

Steady state analysis was conducted for two Mach number cases for comparison; Mach 0.75 where a shock is not created yet, and Mach 0.80 where a shock wave is appearing on the rear part of a wing surfaces.[13] Fig. 6 shows chordwise pressure distribution at 70 % spanwise section at Mach 0.75 of measurement data and CFD analysis results considering the elastic deformation. The correspondence is good. Calculated results at Mach 0.80, Fig. 7, shows a strong shock appearing at the rear wing surface. Fig. 8 shows the overall pressure distributions at two different Mach numbers. Unusually high pressure peaks on both upper and lower surfaces can be observed at "glove" part which sometimes caused numerical trouble in computation. Though we don't have any test data of pressure distribution at the glove part, these analytical results suggest that some discrepancy between calculation and measurement may occur caused by flow separation.

Unsteady calculation and linearized model

Original USTF3 code was extended to calculate the time response of a transonic generalized aerodynamics due to forced oscillation by eigen modes. Calculation was executed at 11-deferent reduced frequencies, from 0.1 to 1.0 in 0.1 step, and 0.05, for Mach number 0.8. The same grid systems were used as in the steady calculation. The computation time was about 0.87 seconds per time step.

Since the calculation was started from zero initial conditions, calculated results have a transient part at the beginning and gradually tends to sinusoidal steady state. For example, Fig. 9 shows the time history of the calculated generalized aerodynamic forces at reduced frequency of 0.5. At reduced frequency of 0.1, at least 3 cycles of computation is necessary to get the steady state solution. Total computing time amounts to 9360 time steps which consumed 8,098 sec of CPU time. At higher frequency, much more cycles are needed to get steady solution so that the total time steps are almost the same. The computation cycles were thus determined to increase according to the frequency.

When Fourier analysis is conducted to this time response of the aerodynamic forces at a final cycle response, we can obtain frequency response to transonic aerodynamics. In Fig. 10, the complex plane presentation of 4×5 elements of the computed generalized aerodynamic forces (GAF) are depicted as asterisks connected with dotted lines. Almost all elements are obtained as a smooth curve but with few exception: i.e., "off-diagonal elements" of q31, q32, q23 for instance, all are related to third mode. It is conjectured that the third mode may have large deflection at the area of abrupt change of the pressure at shock wave, and shock occurrence is sensitive to the reduced frequency so that the diagram of Fig. 10 shows such an irregular behavior.

Using these describing functions for generalized aerodynamic forces, U-g flutter analysis was conducted. As the result is shown in Fig. 11, the second mode will get into flutter though the predicted flutter speed is much lower than occurred in the test.

By fitting 1st order rational functions as shown in Eq. (5b) to the calculated data, a finite state math model is obtained which is depicted in Fig. 10 as a solid line. Eigen value analysis was done by this model to get another prediction of flutter and its velocity root locus is shown in Fig. 12. The flutter speed is almost the same as predicted by U-g method and the tendency of the locus is also the same which means that the finite dimensional approximation is successful. The problem remained yet is that these flutter speed have discrepancy with the tested data. As pointed out previously, the possible discrepancy between analytical and test pressure distribution may occur by flow separation which may in turn cause the flutter speed discrepancy. We therefore decided to introduce the reduction factor to the calculated aerodynamic forces intending to express the aerodynamic

inefficiency caused by flow separation. Fig. 13 shows the speed root locus for the model with the reduction factor of 0.338, while Fig. 14 shows the root locus for the model based on subsonic lifting surface theory of Doublet Point Method (DPM) where the reduction factor of 0.305 was used. Though apparent difference is the relation of the 1st and 2nd mode to flutter, it is notified that the resulting flutter mode is not so much different to each other.

Robust stability control synthesis

Sketch of the synthesis method

Robust stability control design based on coprime factors approach was applied to this wing model and the reduced order controller was obtained by the residualization method which yielded control laws with a certain level of robustness.[14] The design process combines classical open-loop shaping principle with an H_∞ robust stabilization problem in the normalized coprime factors framework. Main contents of the procedure is summarized here; the detailed process is stated in Reference 14.

Let the nominal plant model $G(s)$ have a normalized left coprime factorization such as,

$$G(s)=M(s)^{-1}N(s)$$

where $N(s)N(s)^* + M(s)M(s)^*=I$ for all s, and $N(s)$, $M(s)$ are asymptotically stable proper real rational functions and $M(s)^*= M(-s)^T$. The uncertainties in the plant can be represented in terms of additive stable perturbations $[\Delta N(s), \Delta M(s)]$ to the factors in a coprime factorization of the plant as shown in Fig. 15.

Let a minimal realization of a proper plant be $G(s) = (A, B, C, D)$, and let $X, Z>0$ be the positive definite solution to the following algebraic Riccati solutions

$$A_X^*X + XA_X - XBS^{-1}B^*X + C^*R^{-1}C = 0 \qquad (9)$$

$$A_ZZ + ZA_Z^* - ZC^*R^{-1}CZ + BS^{-1}B^* = 0 \qquad (10)$$

where A_X and A_Z are

$$A_X = A - BS^{-1}D^*C$$

$$A_Z = A - BD^*R^{-1}C$$

then, for a given $0 < \varepsilon < \varepsilon_{max}$, the state space realization of a central controller K_ϕ can explicitly be given, using Doyle's notation, as

$$K_\phi(s) = \left[\begin{array}{c|c} A^c+\varepsilon^{-2}W_1^{-1}ZC^*(C+DF) & \varepsilon^{-2}W_1^{-1}ZC^* \\ \hline B^*X & -D^* \end{array}\right] \qquad (11)$$

$$S = I + D^*D, \quad R = I + DD^*, \quad A^C = A + BF$$
$$W_1 = I + (XZ - \varepsilon^{-2}I), \quad F = -S^{-1}(D^*C + B^*X)$$

The maximum stability margin, ε_{max}, is given as

$$\varepsilon_{max} = [\, 1 + \lambda_{max}(ZX) \,]^{-1/2} \qquad (12)$$

where $\lambda_{max}(ZX)$ is a maximum Hankel norm for the nominal plant and is a function of ZX.

In order to incorporate performance objectives in the design process, input and output shaping functions $W_i(s)$, $W_o(s)$ are introduced just before and after the normal plant. The extended plant is thus given as $G_e(s) = W_oGW_i(s)$ so that feedback controller can be given as

$$K_e(s) = W_iK_\phi W_0(s) \qquad (13)$$

where a controller K_ϕ is obtained from Eq. (11) by substituting a plant dynamics $G(s)$ with $G_e(s) = (A_e, B_e, C_e, D_e)$. The maximum stability margin for an extended plant can be expressed accordingly as

$$\varepsilon_{emax} = [\, 1 + \lambda_{max}(Z_eX_e) \,]^{-1/2} \qquad (14)$$

Control law design

Control law was designed at the design dynamic pressure of 32.4 kPa, 20% higher than the open loop flutter. According to the previous experience obtained by the model based on subsonic aerodynamics[5], almost the same structure of the control component was adopted. Order of the shaping function was set three and low pass filter of 30 Hz cut-off frequency was introduced in order to prevent the higher mode spill over. The order of the extended plant is increased to 22: 14 from the original plant, 6 from the shaping function, 2 from the low pass filter. Direct application of the design procedure produced 22th order controller, the same order as the extended plant. Sensitivity and complimentary sensitivity for full order controller were estimated by changing the shaping function gain and good performance was obtained with the gain value of 1 as shown in Fig. 16. Order reduction method of residualization with a balanced truncation approximation process[14] was then applied to this full order controller. Order reduction to 7th order was found most efficient in the sense that the reduction error in frequency response of the controller between successive order reduction is minimized.

The robust performance of the controller was estimated by changing the two important parameters, 1st mode and 2nd mode stiffness. Table 1 shows the results. It was found that the controller is robust against the first mode variation, while it is very sensi-

tive to change of the second mode stiffness. The controller will lose the stability even at the original flutter dynamic pressure if the second mode stiffness changes 10%. Table 2 shows the same diagram for another controller (CT31-171) which was designed for the model based on subsonic DPM. In this diagram, the first mode change does not degrade the control performance but reduction of the second mode stiffness degrades the control performance just like the above results for USTF3 model. The sensitivity chart of this control law shown in Fig. 17 shows that it maintains excellent robustness and noise reduction performance. Almost similar control law was recently tested in the wind tunnel and succeeded to demonstrate its effectiveness by recovering the flutter once occurred when the control loop was disengaged. Fig. 18 shows these situation in the time chart. Considering the test results and the related chart for the controller CT31-171 and newly designed USTF3 controller, it can be concluded that the present controller will realize certain level of flutter speed increase in the wind tunnel test.

As future research subjects, wind tunnel test verification of the effectiveness of the newly designed control law should be carried out. Flutter simulation using USTF3 function by implementing the control law should also be treated.

Summary

A transonic full potential code, USTF3, was extended to calculate the generalized aerodynamic forces due to eigen mode oscillation for reduced frequency range from 0.05 to 1.0. Fourier series analysis was then applied to final cycle of calculated time history of GAF to get a describing function. Linearized aerodynamic model was obtained by fitting a finite state model to the aerodynamic describing function. By implementing this model, linearized math model for aeroelastic wind tunnel model was obtained. In order to compensate possible modeling error, the H_∞ loop-shaping method with the normalized left coprime factors approach was applied to provide a stability robustness against model uncertainty. The sensitivity analysis conducted for the resulting 7th-order controller exhibits robustness. Comparable performance with the previous control laws designed on the basis of subsonic lifting surface method was obtained by the present model.

Acknowledgement

Authors would like to appreciate Professor Isogai, Kyushu University, for his permission for extending and support in using his USTF3 code.

References

1. Matsushita, H., "NAL Research Activities on Active Control of Aeroelastic Systems," *Proceedings of 31st JSASS Aircraft Symposium*, Tokyo, Japan, 1993, pp.436-439.
2. Isogai, K., "On the Transonic-Dip Mechanism of Flutter of a Sweptback Wing," *AIAA Journal*, July 1979, pp.793-795.
3. Isogai, K., "Transonic Dip Mechanism of Flutter of a Sweptback Wing: Part II," *AIAA Journal*, Vol. 19, No. 9, 1981, pp.1240-1242.
4. Dowell, E. H., "Nonlinear Aeroelasticity," Chapter 4, Vol. 5: *Structural Dynamics and Aeroelasticity*, Noor, A. K. and Venneri, S. L., ed., ASME, 1993, pp. 213-239.
5. Matsushita, H., Hashidate, M., Saitoh, K., Ando, Y., Fujii, K., Suzuki, K. and Baldelli, D. H., "Transonic Flutter Control of a High Aspect Ratio Wing: Mathematical Modeling, Control Law Design an Wind Tunnel Tests," *Proceedings of 19th ICAS*, Anaheim, 1994, pp.2070-2079.
6. Saitoh, K., Matsushita, H., Hashidate, M. and Baldelli, D. H., "Active Flutter Suppression of a Flexible Wing in Transonic Region," *Proceedings of 2nd MOVIC*, Yokohama, 1994, pp.581-586.
7. Baldelli, D. H., Ohta, H., Matsushita, H., Hashidate, M. and Saitoh, K., "Flutter Margin Augmentation Synthesis Using Normalized Coprime Factors Approach," *J. Guidance, Control and Dynamics*, Vol. 18, No. 4, 1995, pp. 802-811.
8. Batina, J. T. and Yang, T. Y., "Application of Transonic Codes to Aeroelastic Modeling of Airfoils Including Active Controls," *J. Aircraft*, Vol. 21, No. 8, 1984, pp. 623-630.
9. Isogai, K. and Suetsugu, K., "Numerical Simulation of Transonic Flutter," NAL TR-726T, Aug. 1982.
10. ACT Study Group, "Gust Load Alleviation of a Cantilevered Rectangular Elastic Wing. — Wind Tunnel Experiment and Analysis," NAL TR-846, 1984, in Japanese.
11. Bisplinghoff, R. L., Ashley, H. and Halfman, R. L., *Aeroelasticity*, Addison-Wesley Publishing Co., 1955.
12. Yonemoto, K., Akatsuka, T., Hiraoka, K. and Mito, S., "Transonic Flutter Calculation Method and Wind Tunnel Test Study of High Aspect Ratio Wing," KHI Technical Report, No. 105, 1990, in Japanese.
13. Saitoh, K., Hashidate, M., Matsushita, H. and Kikuchi, T., "Elastic Deflection Effects on Transonic Aerodynamics of a Flutter Wing Model with Control Surfaces," AIAA Paper 95-3926, 1st AIAA Aircraft Engineering, Technology, and Operations Congress, Los Angeles, Sept. 19-21, 1995.
14. Baldelli, D. H., Ohta, H. and Matsushita, H., "Robust Stabilization of an Aeroelastic Wing Model using Normalized Coprime Factors Approach," The Proceedings of the 31st JSASS Aircraft Symposium, Tokyo, 1993, pp.74-77.

Table 1 The sensitivity of closed loop flutter dynamic pressure due to parameter changes (USTF3 controller)

ω_1 ω_2	-10%	Nom.	+10%
-10%	25.05	36.60	20.36
Nom	23.97	36.90	20.02
+10%	22.80	36.98	19.65

Table 2 The sensitivity of closed loop flutter dynamic pressure due to parameter changes (DPM controller)

ω_1 ω_2	-10%	Nom.	+10%
-10%	29.55	38.22	53.65
Nom	28.73	37.73	45.39
+10%	27.82	37.13	38.71

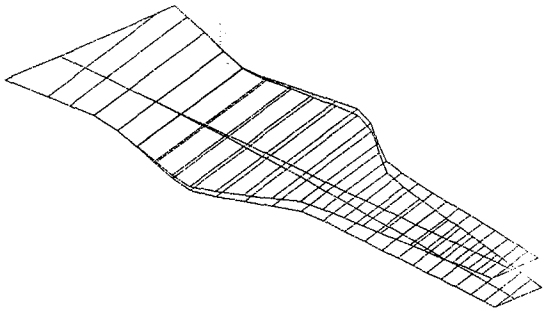

(a)1st mode (f=12.5 Hz)

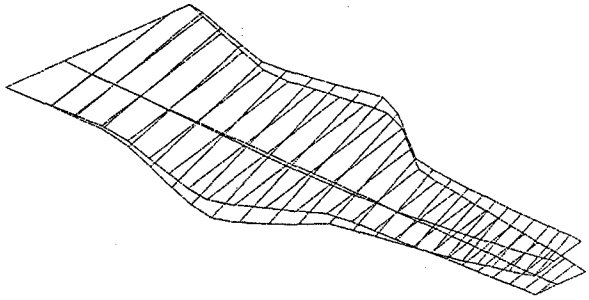

(c)3rd mode (f=44.0 Hz)

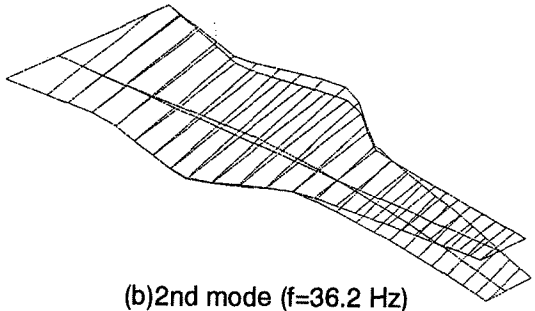

(b)2nd mode (f=36.2 Hz)

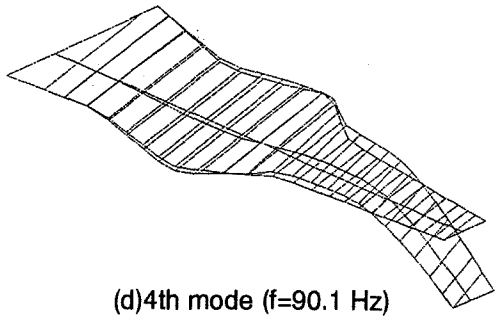

(d)4th mode (f=90.1 Hz)

Fig.2 First four elastic modes

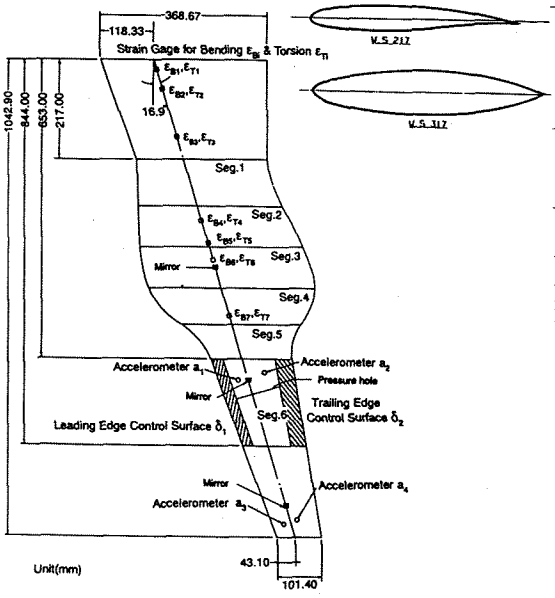

Fig.1 High aspect ratio wing model

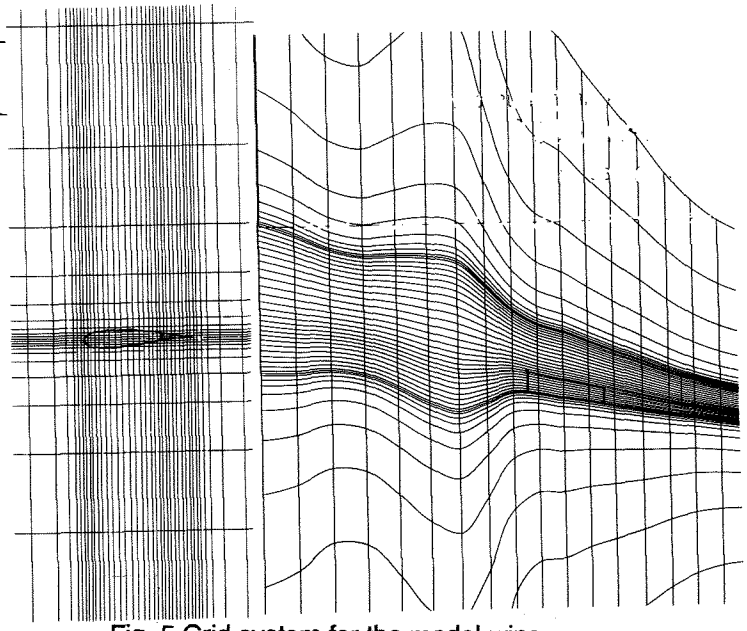

Fig. 5 Grid system for the model wing.

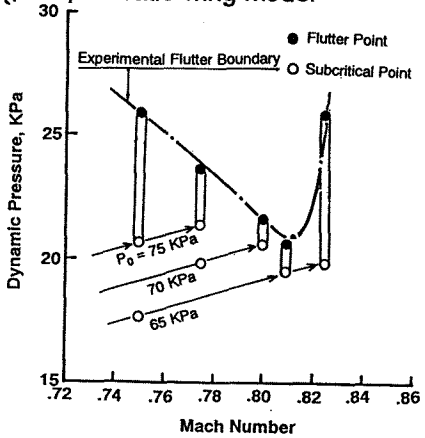

Fig. 3 Transonic dip

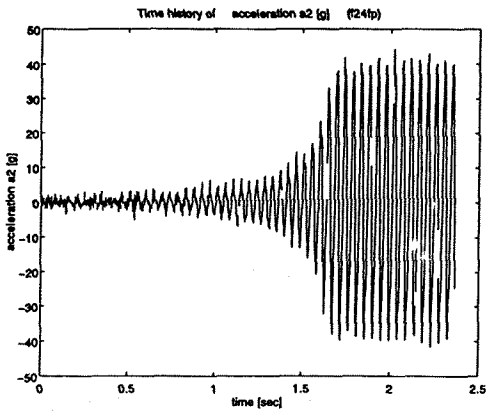

Fig. 4 Limit cycle oscillation of the model

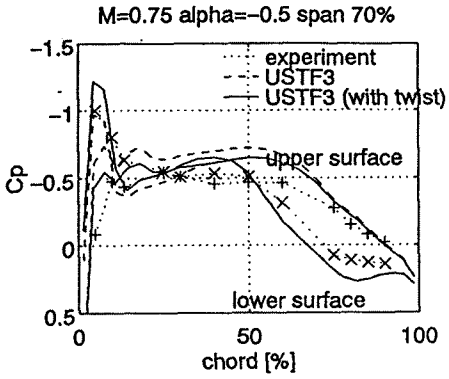

Fig. 6 Chordwise pressure distribution at 70% span(M=0.75)

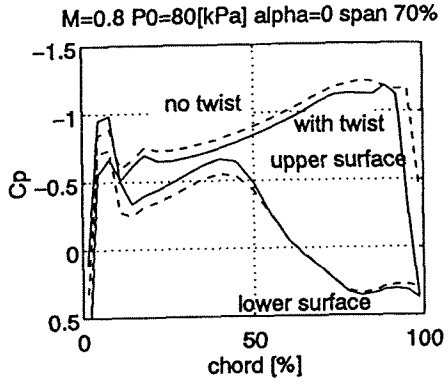

Fig. 7 Computed chordwise pressure distribution(M=0.8)

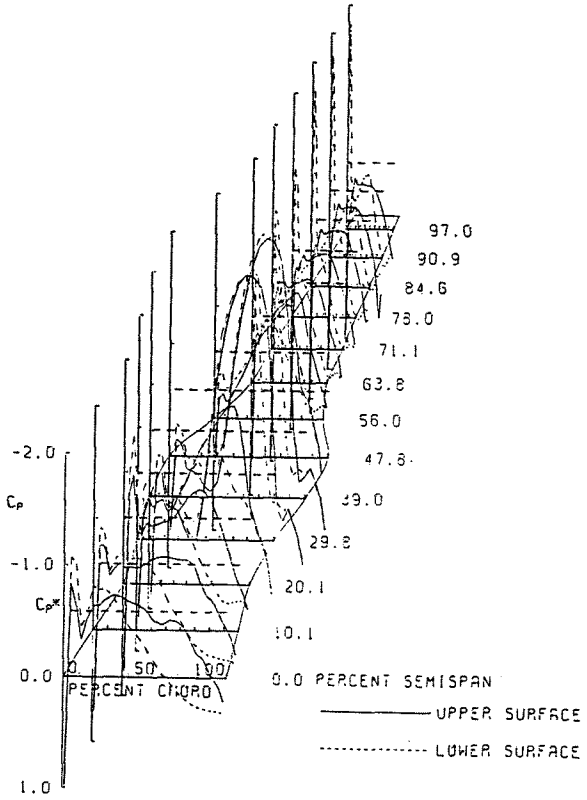

Fig. 8 Static pressure distribution (a)M=0.75

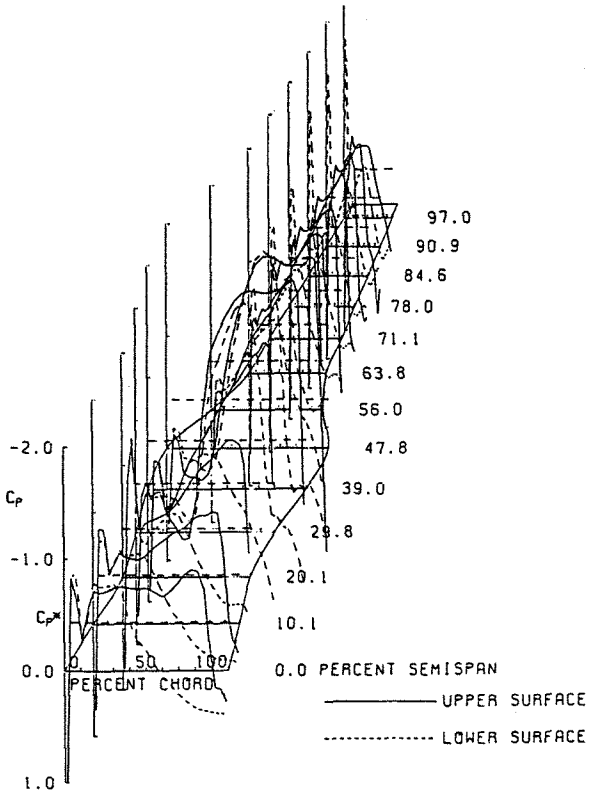

(b)M=0.8

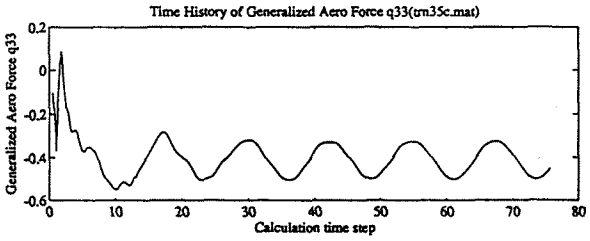

Fig. 9 Time history of the calculated generalized aerodynamic force (Mach=0.8, k=0.5)

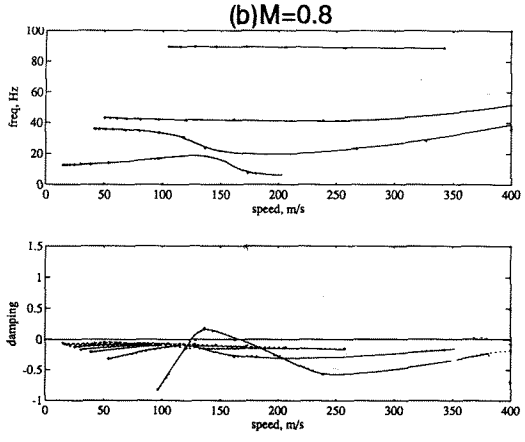

Fig. 11 U-g plot

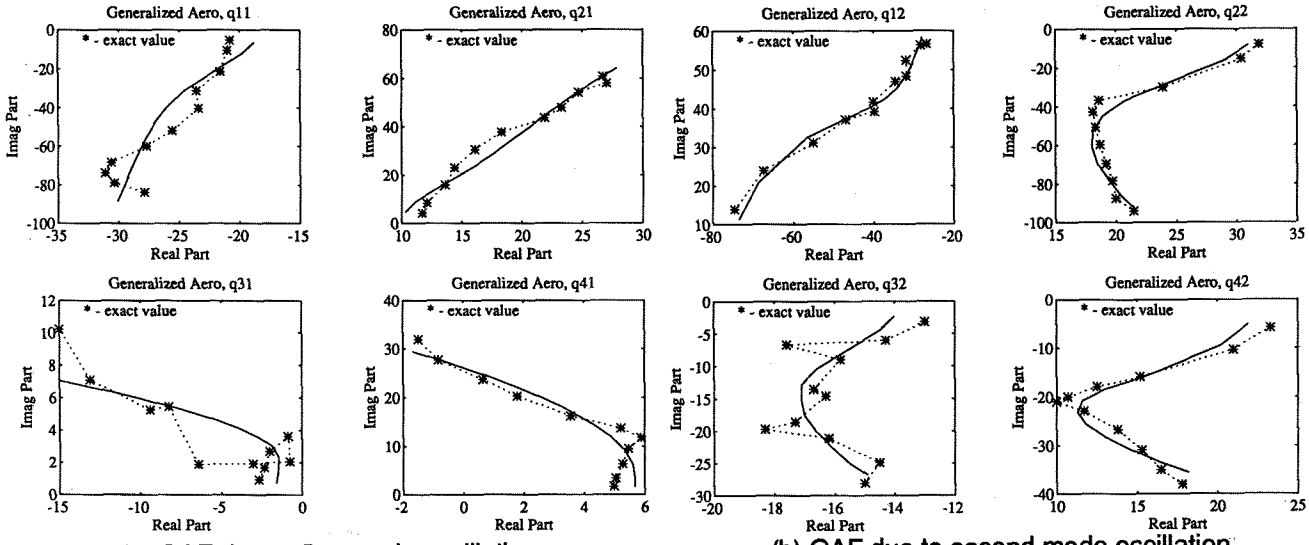

(a) GAF due to first mode oscillation

(b) GAF due to second mode oscillation

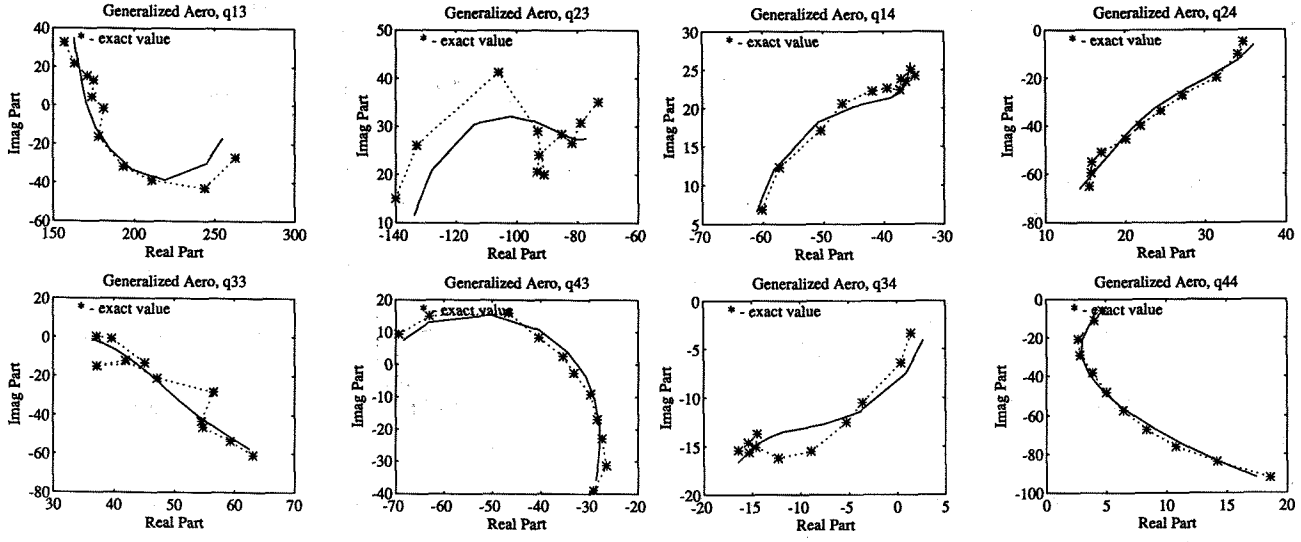

(c) GAF due to third mode oscillation

(d) GAF due to fourth mode oscillation

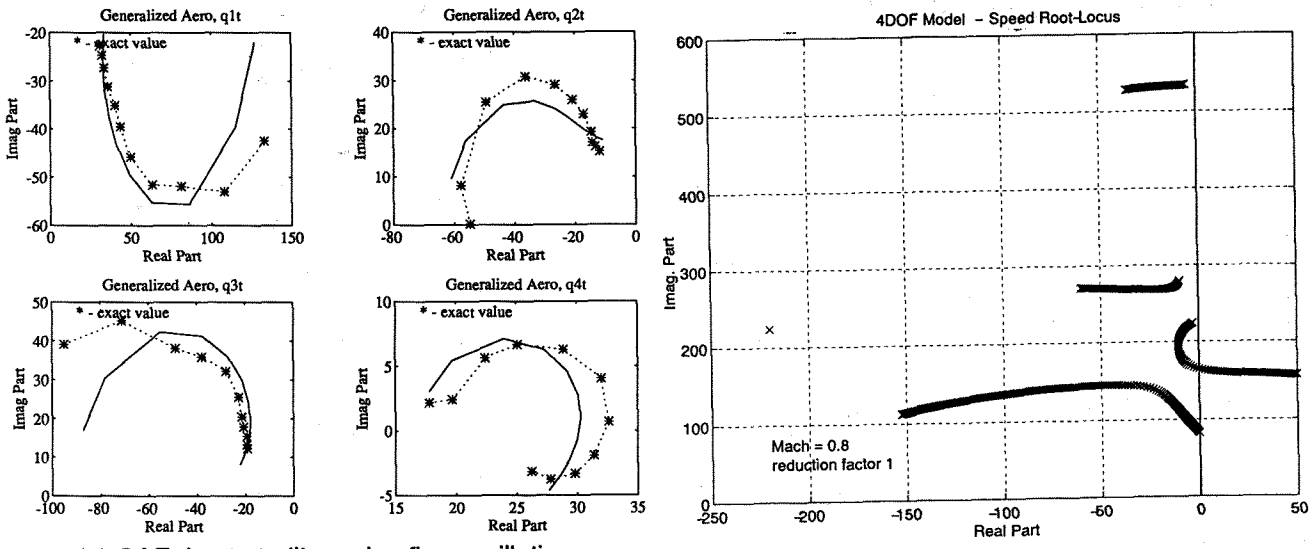

(e) GAF due to trailing edge flap oscillation

Fig. 10 Generalized aerodynamic forces

Fig. 12 Speed root locus (Original model)

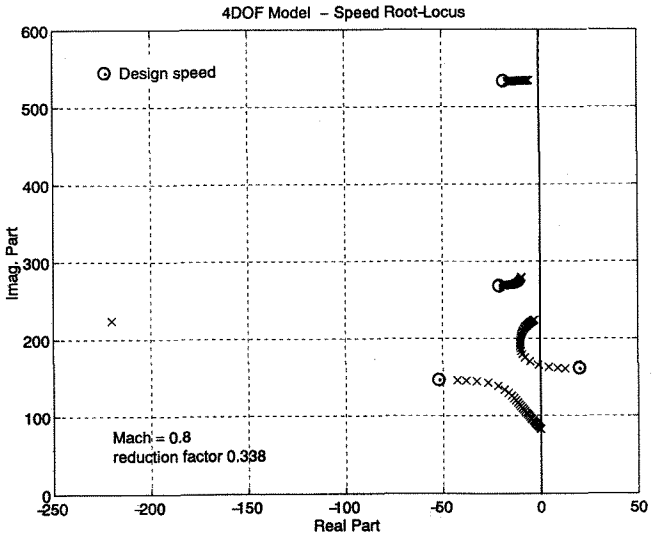

Fig. 13 Speed root locus (USTF3 model)

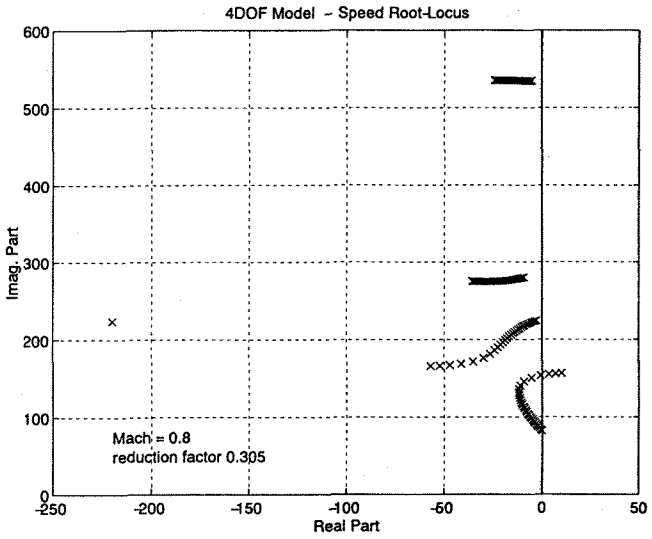

Fig. 14 Speed root locus (DPM model)

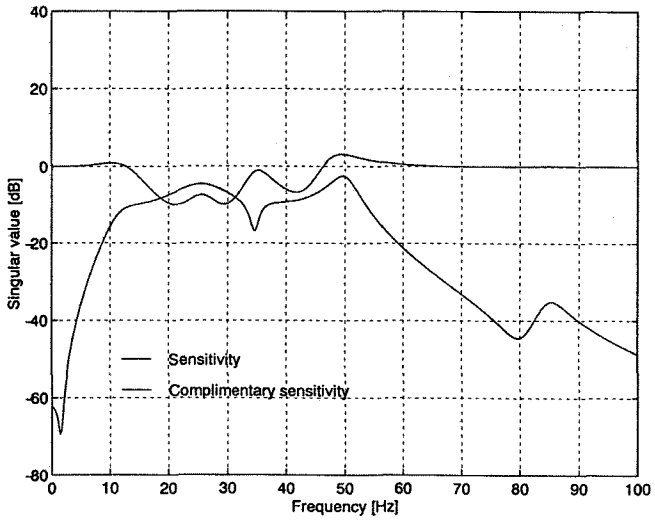

Fig. 16 Sensitivity and complementary sensitivity for full order controller. (USTF3 model)

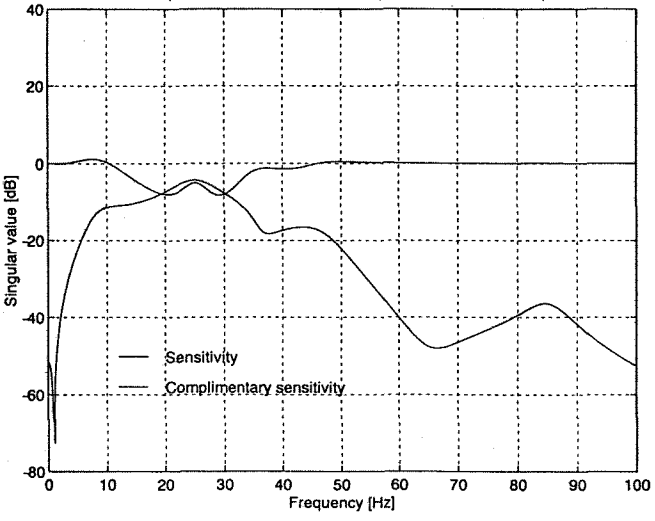

Fig. 17 Sensitivity and complementary sensitivity for full order controller. (DPM model)

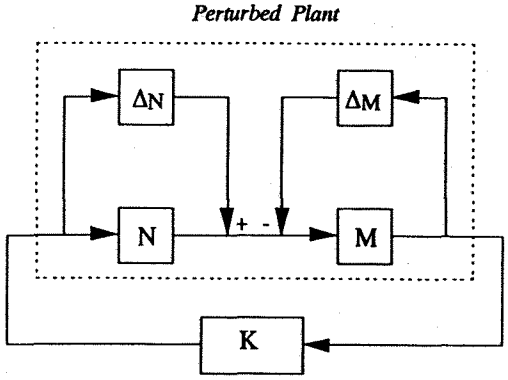

Fig. 15 Coprime factor description and robust stabilization problem

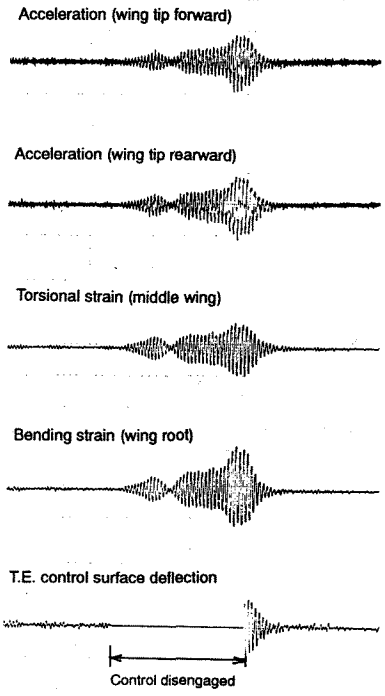

Fig. 18 Time history of successful flutter suppression in the transonic wind tunnel